Cross section measurements of the ^{10}B$(d, n_0)^{11}$C reaction below 160 keV

S. Stave,[1,2] M. W. Ahmed,[1,2] A. J. Antolak,[3] M. A. Blackston,[1,2,*] A. S. Crowell,[1,2] B. L. Doyle,[4] S. S. Henshaw,[1,2] C. R. Howell,[1,2] P. Kingsberry,[1,2] B. A. Perdue,[1,2] P. Rossi,[4,†] R. M. Prior,[2,5] M. C. Spraker,[2,5] and H. R. Weller[1,2]

[1]*Department of Physics, Duke University, Durham, North Carolina 27708, USA*

[2]*Triangle Universities Nuclear Laboratory, Durham, North Carolina 27708, USA*

[3]*Sandia National Laboratories, Livermore, California 94550, USA*

[4]*Sandia National Laboratories, Albuquerque, New Mexico 87123, USA*

[5]*North Georgia College and State University, Dahlonega, Georgia 30597, USA*

(Received 13 March 2008; published 27 May 2008)

New data were taken at the Triangle Universities Nuclear Laboratory to investigate the plausibility of using low energy deuterons and the ^{10}B$(d, n)^{11}$C reaction as a portable source of 6.3 MeV neutrons. Analysis of the data at and below incident deuteron energies of 160 keV indicates an n_0 neutron cross section that is lower than previous estimates by at least three orders of magnitude. In separate runs, deuterons with two different energies (160 and 140 keV) were stopped in a ^{10}B target. The resulting n_0 neutrons of approximately 6.3 MeV were detected at angles between 0° and 150°. The angle integrated yields were used to determine the astrophysical S factor for this reaction assuming a constant value for the S factor below 160 keV. The cross sections reported between 130 and 160 keV were calculated using the extracted value of the S factor. The measured n_0 cross section is several orders of magnitude smaller than previous results, thus eliminating ^{10}B$(d, n)^{11}$C as a portable source of intense neutrons with low energy deuteron beams on the order of tens of microamps. In order to gain insight into the reaction dynamics at these low energies the cross section results have been compared with results from calculations using the distorted wave Born approximation (DWBA) and a detailed Hauser-Feshbach calculation performed by the authors. The angular distribution is consistent with the Hauser-Feshbach calculation suggesting a statistical compound nucleus reaction rather than a direct reaction.

DOI: 10.1103/PhysRevC.77.054607 PACS number(s): 25.45.Hi, 24.10.−i, 24.60.Dr, 29.25.Dz

I. INTRODUCTION

There is an interest in using the ^{10}B$(d, n)^{11}$C reaction as a portable source of 6.3 MeV neutrons for active interrogation of special nuclear materials [1] and explosives [2]. Existing portable neutron sources have energies that are lower [2.5 MeV neutrons from ^{2}H$(^{2}$H, $n)^{3}$He] and so have a reduced penetrating power, or higher [14 MeV neutrons from ^{3}H$(^{2}$H, $n)^{4}$He] and create a strong background by being above the ^{16}O$(n, p)^{16}$N threshold. Neutrons with energies in excess of 5 MeV and below 10 MeV would be useful in material scanning techniques also by being above the threshold for the $(n, n'\gamma)$ reactions on carbon and nitrogen [2].

Previous measurements of ^{10}B$(d, n)^{11}$C reaction rates indicated a large (>10 mb) total neutron cross section at low ($\leqslant$50 keV) energies [3]. However, there are no corroborating data in the energy region below 200 keV. The next sets of available data start near 400 keV [4,5]. There are more data at higher energies [3,6–8] which show a general trend but have rather large discrepancies between themselves. This new experiment extends the cross section measurements to 160 and 140 keV approaching the energies of the Brookhaven experiment [3]. The data were analyzed by assuming a constant astrophysical S factor below 160 keV. This procedure makes it possible to extrapolate the cross section to lower energies which is important for the calculation of the neutron yield from a thick target.

The ^{10}B atom is a 3^+ nucleus while ^{11}C is $3/2^-$. The ^{10}B$(d, n)^{11}$C reaction has a Q value of 6.4650 MeV and ^{11}C has five states which can be populated at our incoming energies [9,10]. For a 160 keV incoming deuteron, the maximum neutron energy of 6.3 MeV occurs when the ^{11}C is left in its ground state. Although the five lower energy neutron groups were in principle populated in our experiment, they could not be observed. This was a result of the fact that during the experimental run, more and more deuterium accumulated in the target and so the ^{2}H$(d, n)^{3}$He reaction produced many background neutrons. Ground state neutrons from the ^{2}H(d, n) reaction have an energy near 3 MeV. As a result the lower energy neutrons from the ^{10}B$(d, n)^{11}$C reaction were lost in the much larger ^{2}H(d, n) peak. Therefore, we were only able to extract a cross section for the n_0 (6.3 MeV) neutrons.

II. EXPERIMENTAL METHOD

The Triangle Universities Nuclear Laboratory (TUNL) atomic beam polarized-ion source produced an unpolarized deuteron beam at 80 keV with about 20 μA on target. An accelerator tube and a high-voltage power supply were used to increase the beam energy an additional 60 and 80 keV for a total beam energy of 140 and 160 keV, respectively. Due to the accelerator tube bias, the beam current was read out using an optical fiber system which isolated the target from ground.

The target was manufactured by Arizona Carbon Foils [11] by evaporating ^{10}B with a thickness of 1.5 μm on a tantalum

*Current address: Oak Ridge National Laboratory, Oak Ridge, Tennessee, USA.

†Current address: Department of Physics of the University and INFN, Padua, Italy.

backing. Tantalum was chosen partly because it has a similar coefficient of thermal expansion to that of ^{10}B [12], thus allowing the thin ^{10}B layer to remain intact despite any beam related heating.

The emitted neutrons were detected using six liquid scintillator neutron detectors located approximately 45 cm from the target and placed at 0°, 23°, 45°, 68°, 113°, and 150°. The detectors were 12.7 cm in diameter and filled with BC-501A liquid scintillator. The threshold for each detector was set at 1.0 times the ^{137}Cs edge. The detector efficiencies for the ^{137}Cs edge threshold setting have been modeled very accurately by the Physikalisch-Technische Bundesanstalt (PTB) group's Monte Carlo programs [13] and have been measured previously at TUNL [14,15]. Pulse shape discrimination (PSD) was used to separate the neutron events from the larger number of gamma-ray events. In the past, this was performed with a long gate/short gate technique. For this experiment, the Mesytec MPD-4 PSD module was used which utilizes a constant fraction discriminator for the rising edge start and a zero-crossing discriminator for tail length. These modules provided very clean separation of the neutrons and gamma rays from an ^{241}Am-Be source and during the experimental runs. The response functions for the neutron detectors were measured previously at TUNL but at higher neutron energies [16]. For this experiment, Monte Carlo codes from PTB were used to generate the response functions at the neutron energies (≈6 MeV) where the measurements were made. The simulated response functions agreed very well with the shape of the neutron distributions measured at higher energies as well as those seen during the experiment.

III. DATA ANALYSIS

After the PSD cuts, the neutron spectrum for each detector was fit using response functions for the n_0 neutrons only. An example of the agreement between the fit and the data is shown in Fig. 1.

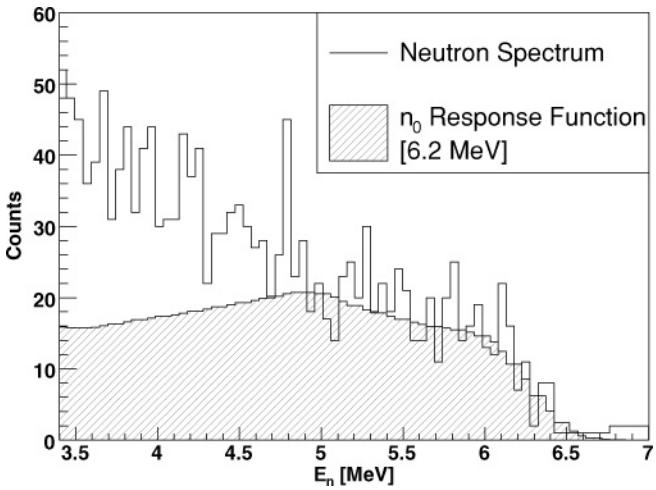

FIG. 1. The neutron spectrum for the ^{10}B$(d,n)^{11}$C reaction at $E_d = 160$ keV, $\theta_{\rm lab} = 45°$ as a function of neutron energy. The fitting procedure used the n_0 group and a region from about 5 MeV to 7 MeV.

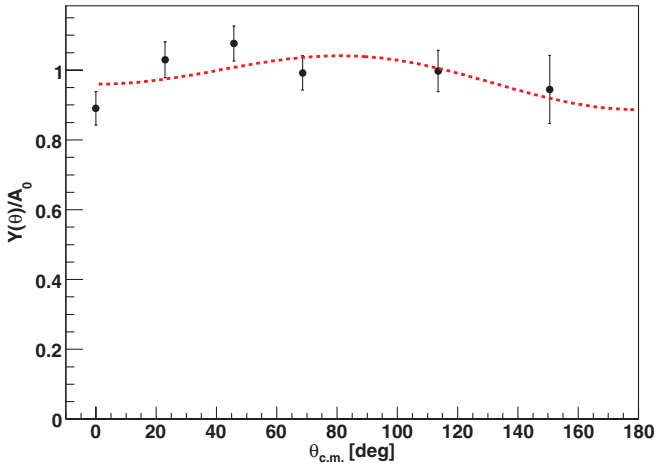

FIG. 2. (Color online) The neutron angular dependent yield divided by A_0 at $E_d = 160$ keV for one run as a function of $\theta_{\rm c.m.}$ and the results of a fit using Legendre polynomials up to second order. The error bars represent statistical errors only.

The fitted response function was then used to calculate the number of neutrons that passed through each detector during the run. Each of these detector yields was then corrected for solid angle, detector efficiency, and dead time, transformed to the center of mass frame and then divided by the charge integrated during the run to give a normalized neutron yield. The normalized neutron yields (which are proportional to the differential cross section) were then fit as a function of $\cos(\theta_{\rm c.m.})$ with Legendre polynomials using the form

$$Y(\theta) = A_0 \left(1 + \sum_{i=1}^{n} a_i P_i(\cos\theta)\right) \tag{1}$$

up to order $n = 2$ (see Fig. 2). This fit allows a simple integration over all angles which then gives the total neutron yield at a given beam energy ($4\pi A_0$). The angle integrated neutron yields were then fit with the S factor formulation to give a total cross section as explained below.

The deuteron beam is very low energy and is stopped completely in the ^{10}B target. Since the cross section is a strong function of energy, it is constantly changing as the deuteron loses energy in the target. The observed neutron yield is the total number of neutrons integrated from the full beam energy down to zero. It can be written as

$$Y(E_d) = C \int_{E_d}^{0} \frac{\sigma(E) f}{\mathrm{STP}(E)} dE, \tag{2}$$

where E_d is the deuteron beam energy, $\sigma(E)$ is the energy dependent cross section, f is the atomic fraction of the target (1.0 for this target), STP(E) is the stopping power of the target for deuterons and C is a constant containing conversion factors and the total number of target particles per cm^2.

The total, energy dependent cross section can be written in terms of the astrophysical S factor as

$$\sigma(E_{\rm c.m.}) = \frac{S(E_{\rm c.m.})}{E_{\rm c.m.}} e^{-2\pi\eta}, \tag{3}$$

where η is the Sommerfeld parameter and $2\pi\eta = 31.29 Z_1 Z_2 (\mu/E_{\text{c.m.}})^{1/2}$. Z_1 and Z_2 are the projectile and target atomic numbers, respectively, μ is the reduced mass in amu, and $E_{\text{c.m.}}$ is the center of mass energy in keV.

As is clear in Eq. (3), the S factor formulation allows the rapidly varying exponential part of the cross section to be divided out leaving the constant S factor part behind. The total neutron yields from the 160 and 140 keV energy settings were then fit with these formulas in order to determine a value for the S factor assuming it was constant as a function of energy $[S(E_{\text{c.m.}}) = S_0]$.

For this analysis, the S factor was used as a tool to parametrize the cross section as a function of energy so that the total neutron yield could be calculated as the deuteron loses energy in the ^{10}B. Due to the rapid change of the cross section with energy, most of this yield ($> 90\%$) is from the first 30 keV of energy loss. Therefore, the exact form of the cross section below 110 keV is not critical for the analysis. To confirm this, a test was performed allowing the S factor to vary linearly with energy. The resulting fit had a larger uncertainty for S_0 but found the same cross sections at 160 and 140 keV within the total errors. However, due to the limited energy range used for the fitting of the S factor, the extrapolation outside of the region between 110 and 160 keV is uncertain.

There were two added complications to the experiment. The first was the constantly increasing ^{2}H(d, n) generated neutrons near 3 MeV. Since this cross section is orders of magnitude larger than the ^{10}B(d, n) cross section [17], even a small tail from the ^{2}H(d, n) neutrons can contaminate the n_0 region. The second complication was the steady decrease in the n_0 count rate for a fixed current due to a small amount of material accumulating on the front of the target. The additional material degraded the beam energy thus decreasing the number of neutrons generated. For reference, a layer of carbon only 4 nm thick will degrade a 160 keV beam by almost 1 keV [18].

The idea that carbon was the material accumulating on the target was tested by looking for the protons from ^{12}C$(d, p_0)^{13}$C at the appropriate kinematically determined energies. The protons generated with 2.0 and 4.5 MeV deuterons on ^{12}C were detected using silicon surface-barrier detectors at various angles in vacuum. The presence of the protons at the appropriate energies indicated carbon on the target and the measured cross section indicated the thickness. In addition, the energy loss of the deuterons elastically scattered off the tantalum backing was used to check the thickness of ^{10}B and ^{12}C. Another check utilized the energy loss of the α_0's from ^{10}B$(d, \alpha_0)^8$Be. All the checks confirmed a ^{10}B thickness of 1.5 μm with a final carbon thickness of about 0.3 μm. The carbon was assumed to accumulate at a constant rate proportional to the beam current, an assumption which was verified by the observed variations in yields as a function of total integrated beam on target.

Due to both the accumulation of carbon and the increase with time of the ^{2}H(d, n) background, a new target was placed in the beam periodically and only the first several hours of beam exposure were used for analysis. During that time, the effect of both processes was small. In addition, the energy of the incident deuterons was changed every hour to either 140 keV or 160 keV in order to monitor changes in the neutron yield over time for both energies and also to provide neutron yield ratios where the amount of carbon buildup would not differ significantly from run to run. Table I shows the ratio of the neutron yields for $E_d = 160$ and 140 keV over the first six hours of running along with the predictions based on a constant and linear S factor neglecting the effects of carbon buildup. The linear S factor assumption agrees better with the data but that is due to the extra fitting parameter on a small set of data (six points) and is not necessarily related to any underlying physics. As mentioned above, the extracted angle integrated n_0 cross section is the same within errors for the constant and linear S factor assumptions and the S factor should not be extrapolated very far outside of the energy range of the experiment. However, as will be detailed in the next section, the TUNL data do place constraints on the size of the cross section at lower energy.

TABLE I. The experimental and calculated ratio of yields for hour-long runs with $E_d = 160$ and 140 keV for the first six hours. The calculated ratios take the effect of the thick target into account and the two results are for constant and linear S factors.

	Time (hours)	Calc. const. S	Calc. linear S	Experimental n_0
Y(160)/Y(140)	0–2	3.58	4.07	4.00 ± 0.24
Y(160)/Y(140)	2–4	3.58	4.07	4.38 ± 0.29
Y(160)/Y(140)	4–6	3.58	4.07	3.81 ± 0.27

IV. EXPERIMENTAL RESULTS AND DISCUSSION

The S factor fit described in the previous section was performed using the data obtained at the two different beam energies in the first six hours of running and gave $S = 11420 \pm 230_{\text{stat}} \pm 2600_{\text{sys}}$ keV b. The statistical error in the S factor is about 2%. The systematic error of about 23% is dominated by the detector response function fitting error but also includes effects from solid angle, charge integration, detector efficiency and carbon accumulation. Figure 3 shows the n_0 yield versus deuteron laboratory energy and the constant S factor fit to the data. The other two curves are for reference and show the neutron yields for S factors approximately 50% larger and smaller than the fitted S factor value. The carbon accumulation rate was adjusted to give the best fit and is consistent with the deuteron elastic scattering energy loss and cross section measurements. As the deuterons travel toward the ^{10}B target, they lose energy passing through the carbon buildup. Since the calculated amount of carbon buildup was different for each of the six one hour long runs, the deuteron energy at the surface of the ^{10}B was different for each run. With time, the deuteron energy was degraded more and more leading to the different "effective" energies seen in Fig. 3.

The cross section was calculated as a function of the deuteron laboratory energy (degraded by the carbon buildup) using the fitted constant S factor (see Fig. 4). At the low energies of interest, our new results are totally inconsistent with the previous measurements of Ref. [3]. However, the previous experiment reports a total neutron cross section and

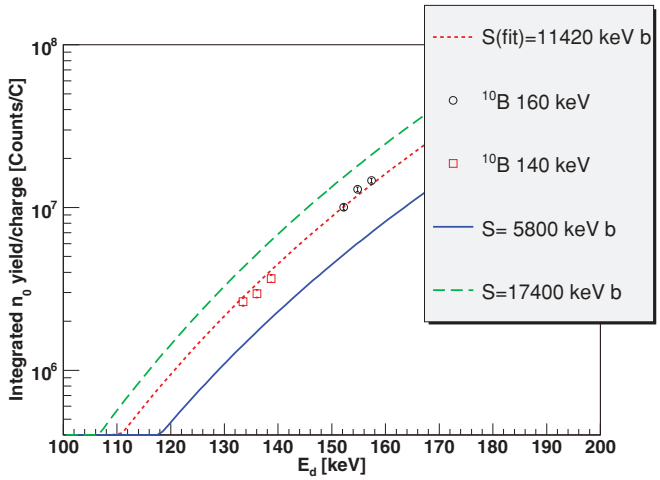

FIG. 3. (Color online) The integrated n_0 yield from the first six hours of running fit with the constant S factor formalism and correcting for thick target effects. The carbon accumulation rate was adjusted to give the best fit. Note that both energy settings are close to the same constant S factor curve.

our result is for n_0 neutrons only. The distorted wave Born approximation (DWBA) and Hauser-Feshbach calculations included in Fig. 4 and detailed below were both used to calculate the n_0 part of the total neutron cross section. The DWBA calculation predicts the n_0 fraction to be approximately 20% while the Hauser-Feshbach calculation predicts approximately 30%. Both calculations predict the n_0 part of the total neutron cross section to be non-negligible and certainly not the several orders of magnitude smaller it would have to be in order to be consistent with the previous data. Furthermore, since the deuteron beam stops in the target, a large cross section at lower energies of the size reported in Ref. [3] would reveal itself through the observation of a larger-than-expected number of neutrons as well as a constant neutron rate at deuteron energies of 160 and 140 keV. The large drop-off in count rate between 160 and 140 keV places a limit on the size of the cross section at lower energies. The cross section for the n_0 channel at and below $E_d = 50$ keV must be less than 30 nb in order to be consistent with the 160 and 140 keV data within the total errors. Even at the few percent level of contribution to the total neutron cross section, this implies a value for the total neutron cross section which is less than a few microbarns at low energies. The disagreement with the previous data can perhaps be resolved with a careful reading of Ref. [3] which indicates that the large cross section results at low energies were at the limit of sensitivity of the experiment. It was an activation experiment and the authors reported seeing no production of ^{11}C at the low energies.

The results of the fit to the angular distribution (Fig. 2) using Eq. (1) were $A_0 = 1.16 \pm 0.035$, $a_1 = 0.036 \pm 0.050$, and $a_2 = -0.077 \pm 0.054$. Since a_1 is consistent with zero, we conclude that there is no fore-aft asymmetry. In addition, the very small value for a_2 indicates an almost isotropic distribution which is evidence for this reaction being dominated by a statistical compound nucleus reaction mechanism. The angular distribution at $E_d = 140$ keV is similar.

To further investigate the direct reaction versus compound nucleus issue, a distorted wave Born approximation (DWBA) calculation was performed using DWUCK [19] with potentials from [20] ($^{12}\mathrm{C} + n$ to represent the $^{11}\mathrm{C} + n$ channel [21], $^{10}\mathrm{B} + p$ [22], and $^{10}\mathrm{B} + d$ [23]). The spectroscopic factor for the ground state of ^{11}C was taken to be $S_{d,n} = 1.12$ [9]. The results of the calculation are shown in Fig. 5 along with a calculation based upon the assumption of a stripping reaction described using the plane wave Born approximation (PWBA). In this model the cross section is assumed to behave according to

$$\sigma(\theta) \propto |j_1(k(\theta)R)|^2 \tag{4}$$

with $k = p_T/\hbar$, where p_T is the transferred momentum and contains the θ dependence, R is the effective radius at which

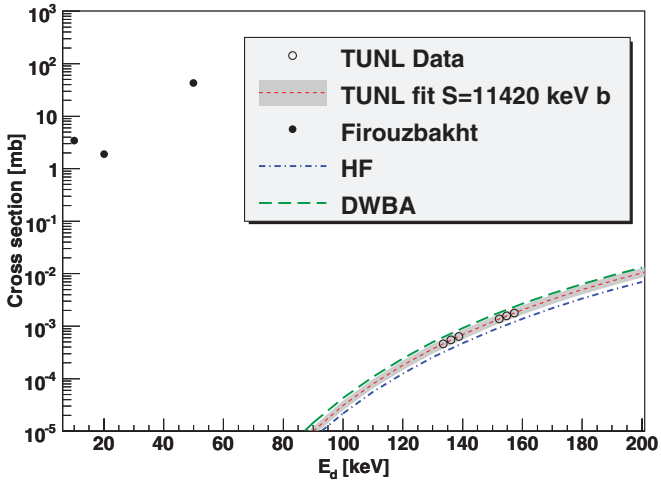

FIG. 4. (Color online) The shape of the $E_d = 160$ keV n_0 differential cross section from the data compared with a Hauser-Feshbach (H-F) calculation, a distorted wave Born approximation (DWBA) calculation and a plane wave Born approximation (PWBA) direct reaction calculation. The results for $E_d = 140$ keV are similar.

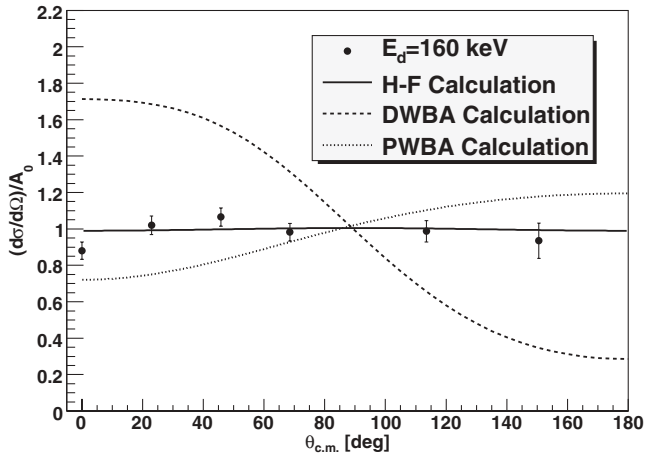

FIG. 5. The new TUNL data (open circles) along with the constant S factor fit (dashed line) and the statistical and systematic errors added in quadrature (gray band). Also included are the Hauser-Feshbach (HF) and DWBA calculation results as a function of energy. The three lower energy data points (solid circles) are total neutron cross sections from Ref. [3].

TABLE II. Comparison of the total n_0 cross sections at $E_d =$ 160 and 140 keV from the constant S factor fit, a detailed Hauser-Feshbach (H-F) calculation, and from a DWBA calculation using DWUCK.

E (keV)	Measured n_0 cross section (μb)	Calculated H-F (μb)	Calculated DWBA (μb)
160	$2.04 \pm 0.03 \pm 0.47$	1.39	2.67
140	$0.69 \pm 0.01 \pm 0.16$	0.48	0.92

the reaction is assumed to occur and $j_1(\theta)$ is the first spherical Bessel function. The PWBA calculation indicates an angular distribution which is backward peaked while the DWBA calculation is forward peaked. The fact that the angular distribution in Fig. 2 is much flatter and does not appear to have the back- or forward-angle peaking is further evidence for this being a statistical compound nucleus reaction and not a direct reaction.

Given the evidence of a compound nucleus reaction, a detailed Hauser-Feshbach calculation was performed to calculate the total n_0 cross section as well as the angular dependent of the cross section. The calculation included all the open two-body outgoing particle channels for 160 and 140 keV deuterons (elastic $^{10}\mathrm{B} + d, ^{11}\mathrm{C} + n, ^{11}\mathrm{B} + p$, and $^{8}\mathrm{Be} + \alpha$) and used their known spins, parities and energies from Refs. [9,10]. The transmission coefficients were calculated using SCAT2 [24] and optical model parameters from: [21] ($^{12}\mathrm{C} + n$), [25] ($^{11}\mathrm{B} + p$), [23] ($^{10}\mathrm{B} + d$), and [26] ($^{9}\mathrm{Be} + \alpha$). The procedure followed the details of Ref. [27] and included the same optical model potentials used in the DWUCK calculation from above. The optical model potentials had to be chosen very carefully since different potentials, especially for the outgoing $^{11}\mathrm{C} + n$ channel, changed the n_0 cross section by more than an order of magnitude. The problem was resolved by comparing the total neutron inelastic cross section calculated by the optical potentials with scattering data from [28]. For potentials with initial energies near the energy required for the outgoing channel, the potential of Ref. [21] agreed the best with data. Table II and Fig. 4 show that the detailed Hauser-Feshbach calculation yields a total n_0 cross section which is about 30% lower than our experimental result while the DWBA results are about 30% higher. However, the energy dependence of both calculations is consistent with the constant S factor fit throughout the experimental energy range, as illustrated in Fig. 4. Additionally, the Hauser-Feshbach calculation provides a ratio of the P_2 to P_0 contribution (the a_2 coefficient) which, for this case, is about -0.01. The Legendre polynomial fit shown in Fig. 2 gave $a_2 = -0.077 \pm 0.054$ which agrees on the sign and is almost within the 1σ error.

V. CONCLUSION

The new result for the $^{10}\mathrm{B}(d, n_0)^{11}\mathrm{C}$ cross section measurement from TUNL yields a value near $E_d = 160$ keV of $\approx 2.0 \pm 0.5$ μb. This value is at least 3 orders of magnitude smaller than the lower energy total neutron cross section data from [3]. As a result, this reaction will not yield an amount of 6.3 MeV neutrons at these incident deuteron energies which could be used in practical applications, at least not with deuteron beam currents on the order of tens of microamps. However, these results are consistent with the predictions of a Hauser-Feshbach treatment of the reaction suggesting a statistical compound nucleus reaction rather than a direct reaction. The angular distributions further corroborate this conclusion.

ACKNOWLEDGMENTS

The authors would like to thank Alex Gurbich for providing his optical model code which was used to calculate transmission coefficients. This work was supported by US DOE Grant Nos. DE-FG02-97ER41033 and DE-FG02-97ER41046 and Sandia National Laboratories LDRD (Laboratory Directed Research and Development). Sandia is a multi-program Laboratory operated by Sandia Corp., a Lockheed Martin Co., for the US DOE's National Nuclear Security Administration under contract DE-AC04-94AL85000.

[1] J. M. Hall *et al.*, Nucl. Instrum. Methods B **261**, 337 (2007).
[2] T. Gozani, Nucl. Instrum. Methods A **353**, 635 (1994).
[3] M. L. Firouzbakht, D. J. Schlyer, and A. P. Wolf, Nucl. Med. Biol. **25**, 161 (1998).
[4] L. C. Feldman and S. T. Picraux, in *Ion Beam Handbook for Material Analysis*, edited by J. W. Mayer and E. Rimini (Academic Press, New York, NY, 1977).
[5] R. W. Michelmann, J. Krauskopf, and K. Bethge, Nucl. Instrum. Methods B **51**, 1 (1990).
[6] K. Von Wohlleben and E. Schuster, Radiochim. Acta **12**, 75 (1969).
[7] B. J. Guzhovskij, S. N. Abramovich, and V. A. Pereshivkin, Vop. At. Nauki i Tekhn. **2**, 55 (1984).
[8] B. Anders, P. Herges, and W. Scobel, Z. Phys. A **301**, 353 (1981).
[9] F. Ajzenberg-Selove, Nucl. Phys. **A506**, 1 (1990).
[10] D. Tilley *et al.*, Nucl. Phys. **A745**, 155 (2004).
[11] Arizona Carbon Foil Co., Tucson, AZ.
[12] D. R. Lide, ed., *CRC Handbook of Chemistry and Physics*, Vol. 87 (The Chemical Rubber Co., Cleveland, OH, 2006), 87th edition.
[13] G. Dietz and H. Klein, *NRESP4 and NEFF4 Monte Carlo Codes for the Calculation of Neutron Response Function and Detection Efficiencies for NE 213 Scintillation Detectors* (Physikalisch-Technische Bundesanstalt, Bundesalle 100, W-3300 Braunschweig, 1982).
[14] D. E. Gonzalez Trotter, Ph.D. thesis, Duke University (1997).
[15] F. Salinas Meneses, Ph.D. thesis, Duke University (1998).
[16] A. Sabourov *et al.*, Phys. Rev. C **73**, 015801 (2006).
[17] D. S. Leonard, H. J. Karwowski, C. R. Brune, B. M. Fisher, and E. J. Ludwig, Phys. Rev. C **73**, 045801 (2006).
[18] H. H. Anderson and J. F. Ziegler, *Hydrogen Stopping Powers and Ranges in All Elements* (Pergamon, London, 1977).
[19] P. D. Kunz, Zero Range Distorted Wave Born Approximation, http://spot.colorado.edu/kunz/DWBA.html.

[20] C. M. Perey and F. G. Perey, At. Data Nucl. Data Tables **17**, 1 (1976).
[21] C. A. Pearson *et al*., Nucl. Phys. **A191**, 1 (1972).
[22] B. Zwieglinski *et al*., Nucl. Phys. **A209**, 348 (1973).
[23] R. N. Maddison, Proc. Phys. Soc. London **79**, 264 (1962).
[24] O. Bersilon, CEA-N-2227 (1981), provided by Alex Gurbich.
[25] H. G. Pugh, D. L. Hendrie, M. Chabre, E. Boschitz, and I. E. McCarthy, Phys. Rev. **155**, 1054 (1967).
[26] R. B. Taylor, N. R. Fletcher, and R. H. Davis, Nucl. Phys. **65**, 318 (1965).
[27] H. Feshbach, in *Nuclear Spectroscopy Part B*, 1st ed, edited by F. Ajzenberg-Selove (Academic Press, New York, 1960), No. 9 in *Pure and Applied Physics*, Chap. 5, pp. 625–669.
[28] D. J. Hughes and R. B. Schwartz, *Neutron Cross Sections* (Associated Universities Inc., Upton, NY, 1958).